

Investigation of Harmonic Current Aggregation in the TBE/Eletronorte Transmission System

Maise N. S. da Silva* Rafael S. Salles* Alexandre Degan***
Carlos A. Duque** Paulo F. Ribeiro*

* *Institute of Electrical and Energy Systems, Federal University of Itajubá, MG, (e-mail: maise.soares@gmail.com; sallesrds@gmail.com ; pfribeiro@ieee.org).*

** *Electrical Engineering Department , Federal University of Juiz de Fora, MG (e-mail: carlos.duque@ufjf.edu.br).*

*** *Transmissoras Brasileiras de Energia Group, Brazil, (e-mail: adegan@tbe.com.br).*

Abstract:

Harmonic distortions are not new problems in electrical power systems. However, electrical networks have undergone several changes in recent decades, such as the wide range of electronic devices (converters, control devices, etc.), and those equipment produce emission of harmonic currents. The investigation of the contribution of several sources of harmonics in power systems is essential, considering that it is a problem of power quality that cannot be neglected. This paper aims to investigate the aggregation of harmonic currents in a 230kV TBE/Eletronorte system. For this, the transmission system was modeled using MATLAB/Simulink software with the typical values provided by TBE. A vectorial analysis was performed for the three-phase system and a sum analyzes of harmonics from different sources on Phase A, to estimate the influence of those current sources on Castanhal and Guama buses, when a harmonic spectrum is present on Vila do Conde and Utinga buses. In both analyzes, a phase angle spectrum of 10 and 20 degrees was applied in the harmonic source of Utinga. The summation analyzes proved to be useful because it can estimate values that harmonic currents can assume, for different conditions, and can be very useful in the planning stage to avoid estimation errors.

Keywords: Harmonic aggregation, Vector analyzes, Summation Methods, Transmission System

1. INTRODUCTION

In the past, distortions in the fundamental waveform were caused, mainly, by large non-linear loads. In this way, many studies have been done, and techniques developed to understand and mitigate this phenomenon's effects. With the advent of electronic devices and the increase in renewable energy sources on the grid, the use of electronic converters and switching based technologies, became the new source of injection of harmonics into the power network (Bollen et al., 2014; Meyer et al., 2014).

Due to the random characteristics of the effects of harmonics, in transmission systems, it is an interest of utilities to carry out studies that ensure their systems' operation to respect the limits of harmonic distortion established by standards. The study of harmonic for multiple loads aggregation is a challenge. Once a set of sources are considered, and the phase angle of those sources is unknown, it is a major issue to predict their effect on the network due to the cancellation or amplification of some harmonic orders (Escudero et al., 2017).

Different summation techniques are proposed for analyzing the aggregation of harmonic sources. In (Medeiros et al.,

2010), the authors suggest an adjustment in the methodology proposed in IEC 61400-21, which uses only the magnitude of each harmonic current source to calculate its sum, since simulations and real measurements suggested significant errors when the methodology proposed in the used standard. Other study states that methodologies based on IEC 61000-3-6 can also lead to incorrect results, regarding the sum of harmonics for grid code compliance, since the phase angle of harmonic orders must be considered. In this way, the authors propose a sophisticated phase-aligned measurement for phase angles of the sources (Eltouki et al., 2018). The article in (Xiao and Yang, 2012) proposes a methodology based on the probabilistic analysis of the harmonic phase angles. The authors then present a universal harmonic summation law for multiple sources of harmonics. Ribeiro (2010) examines the harmonic summation models defined in IEC 61000-3-6 and states that there are difficulties in modeling and representing multiple sources of harmonic currents.

Ribeiro (1985) uses four methods to estimate the sum of harmonics in a hypothetical system, with characteristics of lines typical of a 230kV CHESF system. In this work, five case studies were analyzed, in which the lengths of transmission lines and the phase shift of harmonic

currents injected into the system vary. The author states that despite the uncertainties in magnitude and phase angle of the injected harmonics, the summation methods can estimate the aggregation's real values for multiple harmonic current sources.

This article aims to investigate the aggregation of multiple harmonic current sources in a real TBE/Eletronorte system, modeled with typical values, comparing the results of the vector analysis with the methods proposed by Ribeiro (1985).

The paper is organized as follows: Section 1 provides an introduction and overview of the paper. Section 2 goes over the principles of harmonics and these distortions in transmission systems. Section 3 provides a description of the paper investigation and the system featuring it. Section 4 shows the results of the analysis and discussion. Lastly, section 5 includes the conclusion and review of the paper contributions.

2. HARMONICS DISTORTION IN TRANSMISSION SYSTEMS

For any power system to be operated with good efficiency and performance, the goal is to have voltage, and current waveforms primarily consist of the fundamental frequency, with minimal higher-order frequencies (Shah, 2013). Harmonics are multiple integers of the fundamental power waveforms (50/60Hz). This distortion is caused by an electrical equipment with non-linear current/voltage characteristics or periodically switched loads, which injects current harmonics into the network (Hooijmans, 2005). Consequently, these currents cause harmonic stresses in the impedance of the electrical system. Therefore, harmonic distortions are one of the main issues investigated in power quality.

The Fourier series can describe harmonic distortions, the series is widely used to investigate this phenomenon of power quality.

In the past, most harmonic related problems were caused by large non-linear loads such as arc furnaces, but these roots problems are mitigated (Hooijmans, 2005). However, due to the widespread penetration of electronic devices and renewable generation converters, harmonic distortion problems continue to be present and require further investigation. Below are the main sources for this issue (Eirgrid, 2013; Levačić et al., 2018):

- (1) Power electronics: power converters, rectifiers, variable frequency drivers (VFD), Flexible AC Transmission System Devices (FACTS), battery chargers, inverters, UPS, etc.
- (2) ARC devices: fluorescent lighting, arc furnace, welding machines, etc.
- (3) Saturated ferromagnets: transformers, motors, generators, etc.

At the transmission system level, non-linear components also exist, for instance, the HVDC converters, static VAR compensators, FACTS devices, or power transformers (Wiechowski, 2006). Transmission networks are particularly exposed to harmonic resonances because circuits have low resistance values, and therefore the resonances have

high-quality factors (Dugan et al., 2012). Thus, the need for performing harmonic assessments is becoming even more pronounced as the connection of non-linear devices or loads increases, driven by the integration of renewable energy sources and the connection of new HVDC converters (Val Escudero et al., 2019).

According to Arrillaga et al. (1997), the flow of harmonic currents in the transmission network produces two main effects: the additional power loss caused by the increased r.m.s. value of the current waveform; and the creation of harmonic voltage drops across the various circuit impedance. This second can increase voltage disturbances. The reduction of useful life in transmission cables and increased faults are also pointed out as effects of harmonics, due to the increase in dielectric stress proportional to the increase in harmonic voltage.

It is also possible to observe the effects of harmonic distortion on power systems as a whole and various associated equipment. The amplification of harmonic levels resulting from series and parallel resonances; Degradation of the power factor; Overheating of the phase and neutral conductors; Reduction of efficiency of the generators; Eddy current and hysteresis losses in transformers; Overheating of the system components, like generators, motors and transformers; Interference problem with telecommunication; and Disturbing moments and noise in rotating machines, are some harmonic effects that can be highlighted (Wiechowski, 2006; Dugan et al., 2012; Hameed et al., 2016).

3. PROJECT INVESTIGATION DESCRIPTION

3.1 System Description and Modeling

A typical 230kV system, located in Pará state, is modeled for this study. In the system, represented in Fig. 1, Vila do Conde and Castanhal buses are owned by Transmissoras Brasileiras de Energia S/A - TBE, while the buses Guamá and Utinga, belong to Centrais Elétricas do Norte do Brasil S/A - Eletronorte. The TBE/Eletronorte system, is arranged in a ring configuration and, to perform this study, has an injection of harmonic current in Conde and Utinga bus bars.

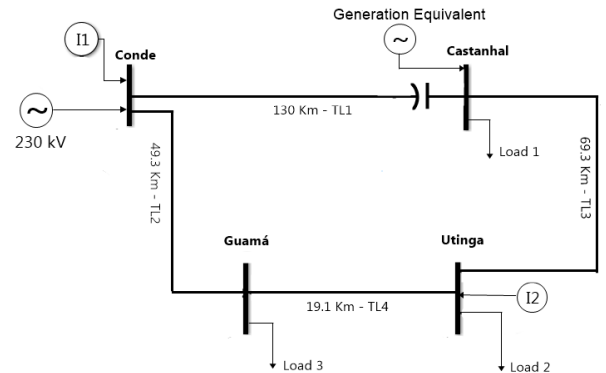


Fig. 1. Transmission System.

The lines length of Vila do Conde-Castanhal, Vila do Conde-Guama, Castanhal-Utinga, and Guama-Utinga, respectively 130km, 49.3km, 69.3km, and 19.1km, and the

characteristics of typical lines were provided by TBE utility. The three-phase system was modeled on Matlab/Simulink using the data acquired from the utility. The software was also used to perform the calculations and to obtain the results. The system modeled on Simulink is represented in Fig. 2

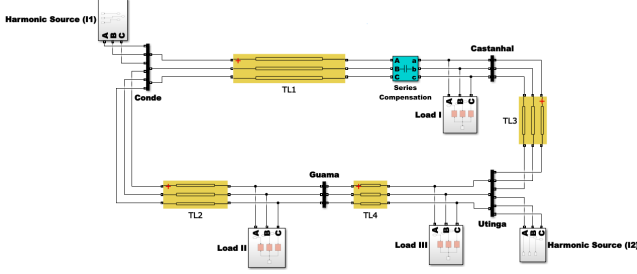


Fig. 2. Simulink Modeled System.

3.2 Current Source for Harmonic Injection

Some techniques of modeling were developed to represent the harmonic sources. The most common and simplest way to represent harmonic behavior on power networks is by considering the loads that generate harmonic distortions as current sources. The harmonic order can have or have no corresponding magnitude and angle represented on a set of current sources (Almeida and Kagan, 2014).

According to (IEEE, 2001), the advantages of this method, besides its straightforward representation, are that the solution is directly obtained (non-iterative), and it has low computational effort. The lag of each harmonic current to the applied voltage, also called phase angle, can be calculated as shown in (1), in which: $\theta_{h_{spc}}$ is the typical phase angle of the harmonic current source spectrum and θ_1 is the phase angle of current on fundamental frequency.

$$\theta_h = \theta_{h_{spc}} + h(\theta_1 - \theta_{1_{spc}}) \quad (1)$$

The estimated phase angle of the current harmonic source was calculated for Phase A in Utinga using the before mentioned 1, as shown in Table 1.

Vila do Conde has a current injection of 1A and phase angle for Phase A equal to -90° , for all harmonic orders. The phase shift (angle between phases) for both buses are equal to $\pm 120^\circ$. Thus, the case studies considered in this paper have the aforementioned injection in Vila do Conde and the spectrum injected in Utinga, with the characteristics above:

- **Case 1:** Injection of 1A in Utinga: $\theta_1 = 0^\circ$ and $\theta_{1_{spc}} = 10^\circ$
- **Case 2:** Injection of 1A in Utinga: $\theta_1 = 0^\circ$ and $\theta_{1_{spc}} = 20^\circ$

Thus, the harmonic spectrum calculated is injected in the Utinga bus, by a set of current sources of odd harmonic orders, up to 35th order, with 1A of magnitude.

3.3 Summation of Harmonic Currents

The investigation aims to estimate the effects of the sum of harmonics from different sources. The harmonics' behavior

Table 1. Typical Phase Angle Spectrum - Phase A

Harmonic Order	Phase Angle Typical Spectrum $\theta_{h_{spc}}$	Case 1 ($\theta_{1_{spc}} = 10^\circ$) θ_h	Case 2 ($\theta_{1_{spc}} = 20^\circ$) θ_h
3	-91.47	-121.47	151.47
5	80.64	30.64	-19.36
7	86.67	16.67	-53.33
9	85.73	-4.27	-94.27
11	-95.35	-205.35	-315.35
13	-96.36	-226.36	-356.36
15	-97.43	-247.43	-397.43
17	81.6	-88.4	-258.4
19	80.42	-109.58	-299.58
21	79.24	-130.76	-340.76
23	-102.33	-332.33	-603.37
25	-103.37	-353.37	603.37
27	-104.76	-374.76	-644.76
29	-106.38	-396.38	-686.38
31	72.22	-237.78	-547.78
33	70.49	259.51	-589.51
35	68.64	-281.36	-631.36

is not deterministic, neither uniform, the variations are unpredictable due to aspects of the sources/system, which can affect the aggregation results. Several methods propose different analyzes to perform this summation. Due to the uncertainty of magnitude and phase angle, a combination of many harmonic sources will typically generate a value other than the arithmetic sum of the maximum values. The methods used in this work to analyze this performance are present in (Ribeiro, 1985), below follow their description and equations. These methods bring, as a result, the magnitude of the current resulting from the sum.

- **Root-Square-Sum (R.S.S):** Corresponds by the significant amplitude and with high probability of occurring.

$$I_{k,h} = \sqrt{\sum_{i=1}^n |I_{i,h}|^2} \quad (2)$$

- **Random Phase (R.P):** Shows a value that has a 37% probability of exceeding the R.S.S.

$$I_{k,h} = \sqrt{\frac{\pi}{2} \sum_{i=1}^n |I_{i,h}|^2} \quad (3)$$

- **Random Phase and Magnitude (R.P.M):** This value has a 5% probability of exceeding the R.S.S. method

$$I_{k,h} = \frac{1}{2} \sqrt{\frac{\pi}{3} \sum_{i=1}^n |I_{i,h}|^2} \quad (4)$$

For all equations above, $I_{k,h}$ is the harmonic current of order h resulting from the summation in the measured bus k , $I_{i,h}$ is the harmonic current of the source i , and n is the number of harmonic sources. The variables are the same for 5.

Thus, this investigation aims to point out the parameters of the summation of harmonic injections in different bars of a transmission system, and the measurements are made in strategic buses. This study seeks to highlight the overlapping behavior of harmonic currents. For the case studied,

all harmonics were specified by magnitude and angle in the three phases. The vectorial summation is the vector sum of the currents injected simultaneously and measured on the same analysis bus. 5 describes this resultant.

$$I_{k,h} = \sum_{i=1}^n I_{i,h} \quad (5)$$

4. RESULTS

4.1 Harmonic Injection Analysis

The harmonic injection aims to analyze the influence of the fundamental current phase angle on harmonic amplification. In this study, as mentioned before, there is a current injection of 1A in Vila do Conde and Utinga buses. Thus the influence of those current spectrums is observed on Castanhal and Guamá buses.

The current magnitudes for Case 1, when the fundamental lag is equal to $\theta_{1_{spc}} = 10^\circ$, can be observed on Fig. 3 and Fig. 4, for Castanhal and Guama buses. On the other hands, the current magnitudes for Case 2, when the fundamental lag is equal to $\theta_{1_{spc}} = 20^\circ$, can be observed in Fig. 5 and Fig. 6.

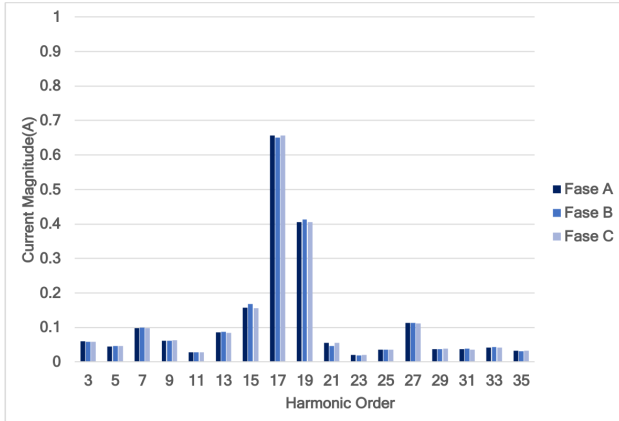


Fig. 3. Harmonic Spectrum Castanhal for Case 1.

The harmonic spectrum on Castanhal bus for Case 1 has harmonic orders varying from less than 0.1A until 0.65A. As can be observed in Table 2, the 17th harmonic order presents the greater value with a magnitude of 0.6571A in Phase A.

Table 2. Castanhal - Case 1

Order	Phase A	Phase B	Phase C
7	0.0973	0.0988	0.9850
15	0.1570	0.1673	0.1565
17	0.6571	0.6500	0.6567
19	0.4049	0.4125	0.4046
27	0.1126	0.1137	0.1112

Guamá presents a greater harmonic spectrum in Case1 when compared with Castanhal. The amplification of the 7th harmonic reach more than 4A. The most significant amplifications on the bus can be seen in Table 3.

In Case 2, the harmonic spectrum of Castanhal has a drop in almost all currents, when compared with Case

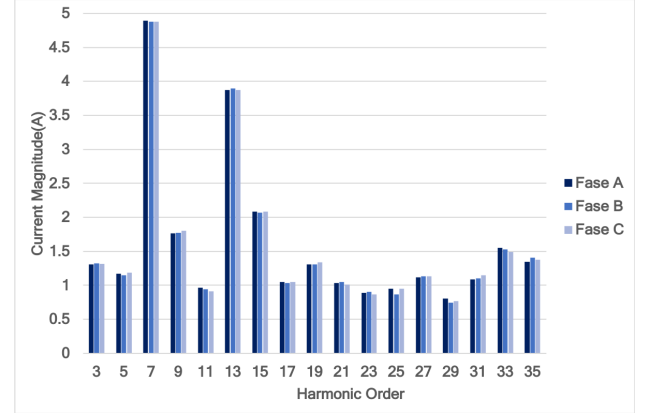


Fig. 4. Harmonic Spectrum in Guamá for Case 1.

Table 3. Guamá - Case 1

Order	Phase A	Phase B	Phase C
7	4.8902	4.8749	4.8752
9	1.7635	1.7697	1.8031
13	3.8723	3.8927	3.8721
15	2.0813	2.0658	2.0842
33	1.5490	1.5306	1.4883

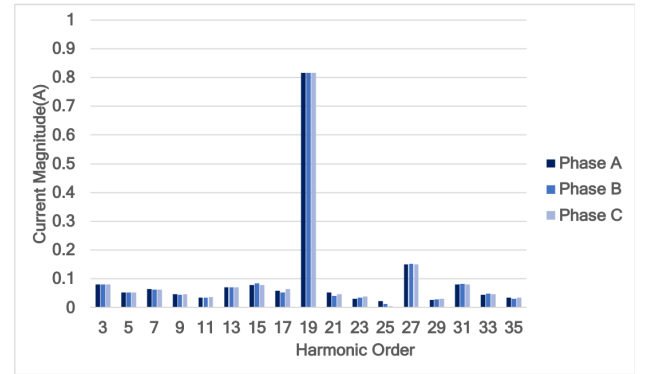


Fig. 5. Harmonic Spectrum Castanhal for Case 2.

1, except for 7th harmonic order, which the current rise up to 0.8163A in Phase A, standing out about the other harmonic orders, and the 27th harmonic order that has a small increase, as described on Table 4.

Table 4. Castanhal - Case 2

Order	Phase A	Phase B	Phase C
3	0.0795	0.0802	0.0810
15	0.0779	0.0841	0.0791
19	0.8163	0.8158	0.8154
27	0.1505	0.1514	0.1492
31	0.0812	0.08244	0.0795

Guamá again presents a greater harmonic spectrum than Castanhal in Case 2. However, it is observed a decrease in current amplitudes when compared with Case 1. In this situation, the harmonic order 13 presents the greatest amplification, reaching more than 3A. The most significant amplifications on the bus, for Case 2, are highlighted in Table 5.

The harmonic injection analysis for the two studied cases points out the relationship between the harmonic spectrum with the phase angle of the fundamental current. For the smaller phase angle, the buses' amplification is, with some

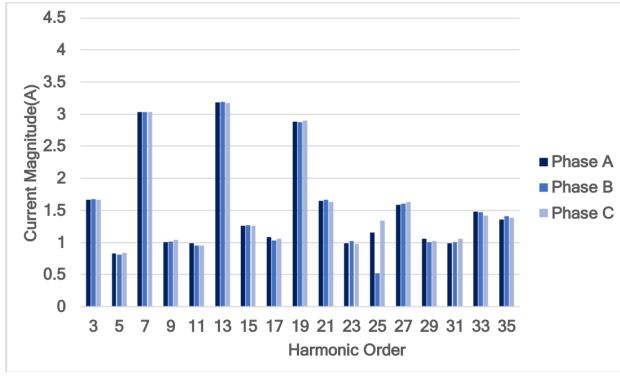


Fig. 6. Harmonic Spectrum in Guamá for Case 2.

Table 5. Guamá - Case 2

Order	Phase A	Phase B	Phase C
3	1.6677	1.6739	1.6666
7	3.0370	3.0289	3.0325
13	3.1820	3.1873	3.1747
19	2.8832	2.8712	2.9025
21	1.6520	1.6649	1.6300

exceptions, greater, while for a greater fundamental lag and the harmonic spectrum magnitude falls. Therefore, from this analysis, it would be possible to affirm that the simple increase of the fundamental current phase angle would be sufficient to decrease the amplitude of the harmonic spectrum. However, other analyzes must be performed to ensure this trend or estimate parameters that can characterize these harmonic currents' uncertain behavior.

For impedance analyzes, it is possible to observe that a greater length, as in the Castanhal-Utinga line (69.3km), causes an increase in the number of resonance points and magnitude when compared with Guamá-Utinga line (19.1 km) as shown in Fig. 7.

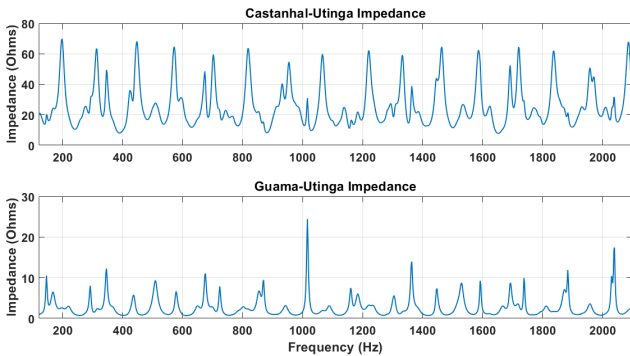


Fig. 7. Castanhal-Utinga/Guama-Utinga Impedance.

4.2 Harmonic Summation Analysis

This study presents a three-phase current injection of 1A up to the 35th harmonic order (2.1kHz) with positive phase sequence at the emitting terminals, Vila do Conde, and Utinga buses are observed. In this way, the effective values of harmonic currents summation from the Vila do Conde and Utinga buses were calculated, by the methods mentioned, in the Castanhal and Guamá buses.

The methods were applied only in phase A of the system for the two cases of phase angle spectrum applied in the harmonic source of Utinga. Fig. 8 and Fig. 9 show the results for Case 1 in Castanhal and Guamá, respectively.

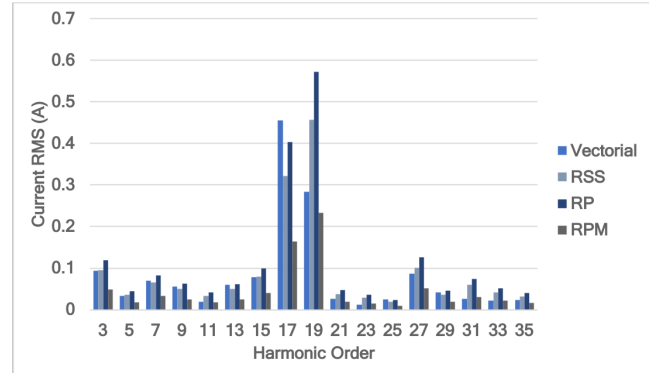


Fig. 8. Summation Results in Castanhal for Case 1.

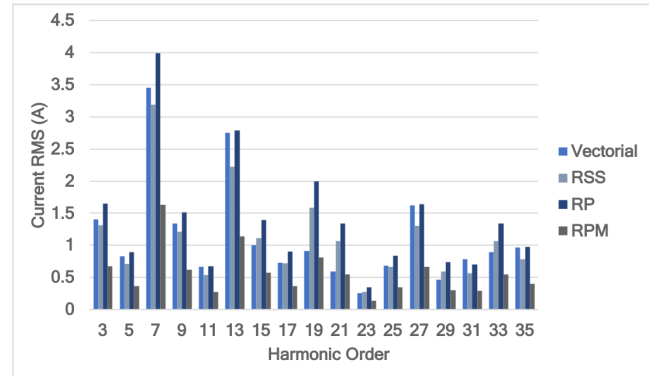


Fig. 9. Summation Results in Guamá for Case 1.

For Case 1, in the Castanhal bus, it is possible to perceive a greater amplification of harmonics of order 17 and 19, taking into account the value of the vector measurement for the values resulting from the sums. On the Guamá bus, the 7th and 13th were the ones with the highest effective value for the sums. In the case of Guamá, harmonics of order 3, 19, and 27 present significant values for the results, which may indicate attention to these orders as well. Table 6 and Table 7 highlight the summation results for the most significant harmonics on each bus.

Table 6. Summation for Case 1 - Castanhal

Order	Vectorial(A)	RSS (A)	RP (A)	RPM (A)
3	0.0942	0.0949	0.1189	0.0485
15	0.0782	0.0791	0.0991	0.0404
17	0.4552	0.3219	0.4035	0.1647
19	0.2843	0.4562	0.5717	0.2334
27	0.0867	0.1006	0.1260	0.0514

Table 7. Summation for Case 1 - Guamá

Order	Vectorial(A)	RSS (A)	RP (A)	RPM (A)
3	1.4007	1.3148	1.6478	0.6727
7	3.4565	3.1862	3.9934	1.6303
13	2.7506	2.2282	2.7926	1.1400
19	0.9134	1.5901	1.9929	0.8136
27	1.6254	1.3067	1.6377	0.6685

In Fig. 10 and Fig. 11 show the results for Case 2 in Castanhal and Guamá, respectively.

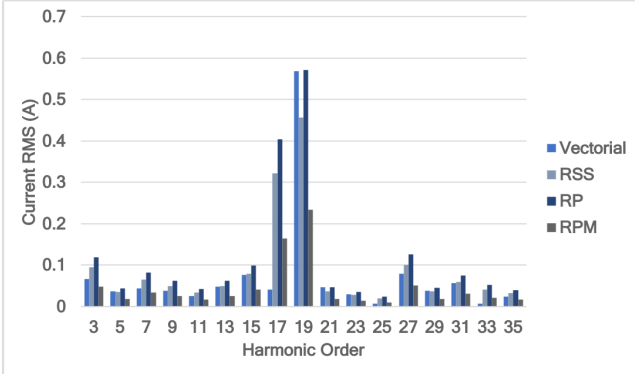


Fig. 10. Summation Results in Casatanhal for Case 2.

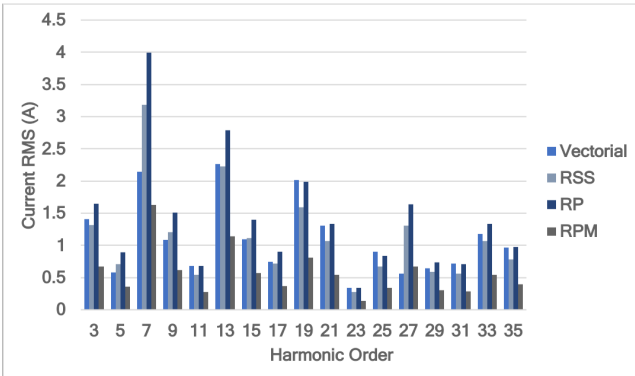


Fig. 11. Summation Results in Guamá for Case 2.

For case 2, on the Castanhal bus, it is possible to perceive a vectorial decrease of the 17th harmonic and even more significant growth of the 19th than Case 1. However, the summation results' values suffer little variation for these harmonic currents, which indicates that singular amplifications can occur, needing to maintain attention to these orders for this system. In this sense, in the Guamá bus, similar variations also occur for the vectorial sum values, a reduction on 7th and 13th harmonics. Still, the summation results show the attention of a potential amplification to the same harmonic orders as in Case 1. Table 8 and Table 9 detail these results.

Table 8. Summation for Case 2 - Castanhal

Order	Vectorial(A)	RSS (A)	RP (A)	RPM (A)
3	0.0661	0.0947	0.1187	0.0484
15	0.0764	0.3219	0.4035	0.1647
17	0.0408	0.3219	0.4035	0.1647
19	0.5692	0.4562	0.5718	0.2334
27	0.0789	0.1005	0.1260	0.0514

Table 9. Summation for Case 2 - Guamá

Order	Vectorial(A)	RSS (A)	RP (A)	RPM (A)
3	1.4131	1.3148	1.6479	0.6727
7	2.1450	3.1862	3.9933	1.6302
13	2.2639	2.2281	2.7926	1.1400
19	2.0149	1.5902	1.9930	0.8136
27	0.5652	1.3065	1.6374	0.6685

These results are important to highlight the role of these summation methods for harmonic currents, as they can estimate parameters that these distortions can assume in the transmission system.

4.3 Alternative Visualization of the Aggregation

This analysis presents only a visualization alternative that contributed to the previous results, allowing a 3-D representation of these harmonic currents in RMS varying in time, due to the vectorial resultant. The use of a color map highlights the harmonic currents that stand out with both sources' contributions. Fig. 12 and Fig. 13 show the 3-D visualization with a color map of Castanhal Bus for Case 1 and Case 2.

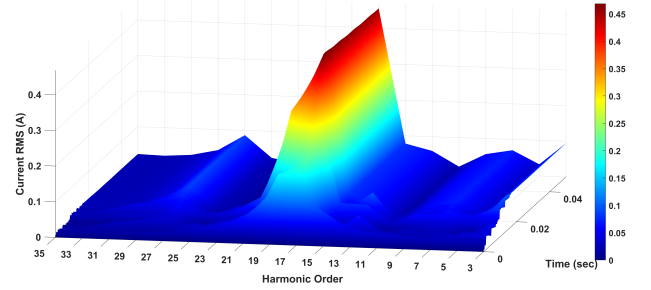


Fig. 12. 3-D Visualization of Harmonic Aggregation in Castanhal - Case 1.

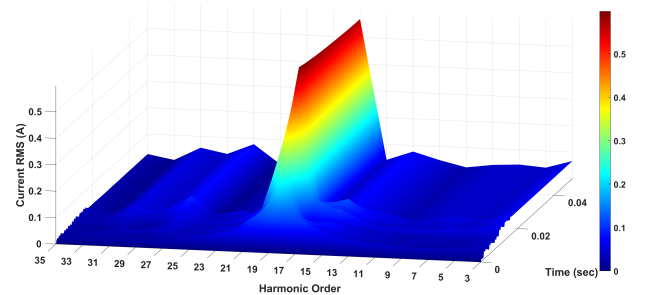


Fig. 13. 3-D Visualization of Harmonic Aggregation in Castanhal - Case 2.

Fig. 14 and Fig. 15 also show this alternative visualization for Case 1 and Case 2, respectively, for Guamá bus. In addition to presenting an alternative way of visualizing the results, these figures highlight the harmonic order through color maps.

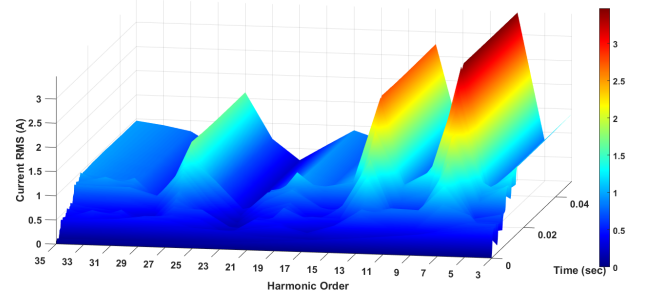


Fig. 14. 3-D Visualization of Harmonic Aggregation in Guamá - Case 1.

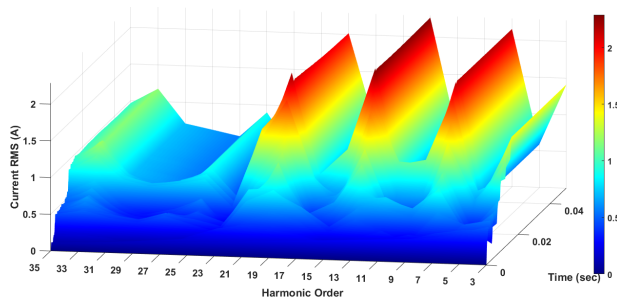


Fig. 15. 3-D Visualization of Harmonic Aggregation in Guamá - Case 2.

5. CONCLUSION

This work investigated the harmonic aggregation in a transmission system. The work was carried out in conjunction with TBE and obtained typical network values for modeling based on a real system. Two methods were used to perform these analyzes. The first sought to analyze the resulting harmonics of injections carried out on buses of the 230kV system and using different typical phase angle spectra. The injection buses were Vila do Conde and Utinga. In the Castanhal and Guamá bus, measurements were made to develop the investigations.

In this first analysis, it was possible to observe the amplification of some harmonic orders and others' attenuation, depending on the phase angle spectrum used. Then, summation methods of harmonic currents were applied to further the investigation. This intended to provide an alternative value that should be interpreted comparatively and based on the harmonic sources' behavior, because it can estimate values that harmonic currents can assume, for different conditions, and can be very useful in the planning stage so that there are no estimation errors. In this way, the methods managed to address the research objectives and assess the most critical harmonic transmission system orders. Finally, a different way of visualizing the results was presented, the value of the currents in RMS varying over time in a 3-D graph with a color map to highlight the amplified orders.

ACKNOWLEDGMENT

This Project is funded by TBE group companies from the R&D ANEEL project, "PD-02651-0016/2018 - Development of a power quality monitoring and a decision taking system for transmission lines." The authors also would like to thank CAPES, CNPq, FAPEMIG, INERGE for providing academic and laboratory support.

REFERENCES

- Almeida, C.F.M. and Kagan, N. (2014). A Novel Technique for Modeling Aggregated Harmonic-Producing Loads. In *The 21st International Conference and Exhibition on Electricity Distribution - CIGRE*, June 2011.
- Arrillaga, J., Smith, B.C., Watson, N.R., and Wood, A.R. (1997). *Power system harmonic analysis*. John Wiley & Sons.
- Bollen, M., Meyer, J., Amaris, H., Blanco, A.M., Castro, A.G.D., Desmet, J., Klatt, M., Kocewiak, L., Rönnberg, S., and Yang, K. (2014). Future Work on Harmonics – Some Expert Opinions Part I – Wind and Solar Power. In *2014 16th International Conference on Harmonics and Quality of Power (ICHQP)*, 904–908.
- Dugan, R.C., McGranaghan, M.F., Santoso, S., and Beaty, H.W. (2012). *Electrical Power Systems Quality, Third Edition*. McGraw-Hill Professional. doi:doi:10.1036/9780071761567.
- Eirgrid (2013). Harmonics Workshop for TSO and DSO customers. URL http://www.eirgridgroup.com/site-files/library/EirGrid/HarmonicsWorkshopPresentationSlides21_11_2013.pdf.
- Eltouki, M., Rasmussen, T.W., Guest, E., Shuai, L., and Kocewiak, L. (2018). Analysis of Harmonic Summation in Wind Power Plants Based on Harmonic Phase Modelling and Measurements. In *17th Int'l Wind Workshop*, October.
- Escudero, M.V., Shore, N., Buchhagen, C., Valade, I., and Ting, D. (2017). *Network Modeling for Harmonic Studies - CIGRE: WG C4/B4.38*. CIGRÉ.
- Hameed, Z., Yousaf, A., and Khan Sial, M. (2016). Harmonics in Electrical Power Systems and how to remove them by using filters in ETAP. In *3rd Int. Conf. on Engineering and Emerging Technologies*.
- Hooijmans, M.A.J.T. (2005). *Harmonic behavior and modeling of grid components and devices*. Master, Eindhoven University of Technology. URL <https://research.tue.nl/nl/studentTheses/>.
- IEEE (2001). Characteristics and modeling of harmonic sources-power electronic devices. *IEEE Transactions on Power Delivery*, 16(4), 791–800. doi:10.1109/61.956771.
- Levačić, G., Župan, A., and Curin, M. (2018). An overview of harmonics in power transmission networks. In *2018 First International Colloquium on Smart Grid Metrology (SmaGriMet)*, 1–6. doi:10.23919/SMAGRIMET.2018.8369828.
- Medeiros, F., Brasil, D.C., Ribeiro, P.F., Cristiano, A.G., and Duque, C.A. (2010). A New Approach for Harmonic Summation Using the Methodology of IEC 61400-21. In *Proceedings of 14th International Conference on Harmonics and Quality of Power - ICHQP 2010*, 1–7.
- Meyer, J., Bollen, M., Amaris, H., Blanco, A.M., Castro, A.G.D., Desmet, J., Klatt, M., Kocewiak, L., Rönnberg, S., and Yang, K. (2014). Future Work on harmonics – Some Expert Opinions Part II – Supraharmonics , Standards and Measurements. In *2014 16th International Conference on Harmonics and Quality of Power (ICHQP)*, 909–913.
- Ribeiro, P.F. (2010). *Harmonic Summation for Multiple Arc Furnaces*, 161–166. Wiley-IEEE Press.
- Ribeiro, P.F. (1985). *Investigations of Harmonic Penetration in Transmission Systems*. Phd thesis, Victoria University of Manchester, England.
- Shah, N. (2013). Harmonics in power systems: Causes, effects and control. Technical report, SIEMENS.
- Val Escudero, M., Lietz, G., Emin, Z., Jensen, C., and Kocewiak, L. (2019). *CIGRE TB 766: JWG C4/B4.38 Network Modelling for Harmonic Studies*. CIGRÉ.
- Wiechowski, W.T. (2006). Harmonics in transmission power systems .
- Xiao, Y. and Yang, X. (2012). Harmonic summation and assessment based on probability distribution. *IEEE Transactions on Power Delivery*, 27(2), 1030–1032.